Chapter 6

Poisson to GOE transition using the distribution of ratio of consecutive level spacings

6.1 Introduction

Quantum systems whose classical counterpart is chaotic will follow one of the three classical ensembles,the Gaussian Orthogonal(GOE), Gaussian Unitary(GUE) or the Gaussian Symplectic(GSE) ensemble depending on the symmetries of the Hamiltonian [100]. For such systems, it is of immense interest to study the chaotic behavior or find out the chaos inducing parameters. Till now we have studied various fluctuation measures to procure information regarding the chaotic nature of many body systems using their spacing statistics like Nearest Neighbor Spacing Distribution (NNSD), the Delta 3 statistics, $1/f^{\alpha}$ behavior for finite interacting many body systems. But in addition to these, we now bring in the present chapter a new method developed recently by Ognaysen and Huse (2007) [101] which enables us to study the spacing statistics of energy levels for nearest neighboring energy levels. This method is called the distribution of ratio of consecutive level spacings, represented by $P(r)dr$.

For this investigation, we consider an interpolating matrix ensemble with a parameter λ giving Poisson ($\lambda = 0$) to GOE ($\lambda \to \infty$) transition. The average of ratio (r) of consecutive level spacings has been analyzed for different matrix dimensions ($d \leq 1000$). The results include (i) introduction of a new transition parameter $\Lambda \sim \lambda^2 d$ giving scaling, (ii) the universal form for the transition curves $\langle r \rangle$, $\langle \tilde{r} \rangle$ versus Λ and (iii) a mapping between $d \times d$ and 3×3 matrix ensembles. Moreover, examples of transition curves are also shown for some of the bosonic and fermionic system discussed in previous chapters. Lastly, introduced are one-dimensional (1D) finite interacting spin-1/2 lattice chains using Heisenberg's XXX and XXZ models and the Poisson to GOE transition is observed therein.

6.2 Ratio of consecutive level spacings : $P(r)dr$ analysis

From the study of nearest neighbor spacing distribution (NNSD), one is able to locate the regime of the system whether integrable or chaotic. This method also justifies the transition from Poisson to Wigner (GOE) observed in finite quantum systems. On similar grounds, researchers in recent years have proposed another such method which not only gives us complete information regarding such quantum transitions but also optimizes the procedure by applying a different approach. It is the procedure of unfolding which is not followed here. Actually this is the most prominent feature that distinguishes this method from the traditional NNSDs. Unfolding of the spectrum can be done in two different ways,one of them being spectral unfolding, i.e. spectrum of each individual member of the ensemble is unfolded separately and the ensemble averaged NNSD is constructed. Alternate method is called as the ensemble unfolding and here a single unfolding function is used for all the members. But it is observed particularly for many-body systems that the above two approaches do not yield same results and there are a lot uncertainties near the end region of the spectrum [102]. Undoubtedly the results achieved so far from NNSD are true and consistent but in

many cases the $P(r)$ distribution serves to be a better measure. This measure was used to quantify the distance from integrability on finite size lattices [103, 104] and also to investigate numerically many-body localization [101, 105, 106, 107]. Also, recently Atas et al [108] derived expressions for the probability distribution of the ratio of two consecutive level spacings for the classical GOE, GUE and GSE ensembles of random matrices. These expressions, called Wigner-like surmises, are shown to be very accurate when compared to numerical calculations in the large matrix size limit. Thus, one may infer that fluctuation measures like $P(r)dr$ measure which are independent of the unfolding procedure are more preferable.

Ognaysen and Huse in 2007 [101] developed the method of ratio of consecutive level spacings, to calculate the spacing statistics of a given system. Let us consider an ordered set of eigenvalues (energylevels) E_n, where $n = 1, 2, ..., d$. The nearest-neighbor spacings is given by $s_n = E_{n+1} - E_n$. Then, the ratio of two consecutive level spacings is $r_n = s_{n+1}/s_n$. The probability distribution for consecutive level spacings as discussed above is denoted by $P(r)dr$. As in the case of NNSD, the Poisson and Wigner distributions were defined, these distributions are redefined or modified for $P(r)$ method. If the system is in integrable domain, then $P(r)$ follows Poisson behavior [denoted by $P_P(r)$],

$$P_P(r) = \frac{1}{(1+r)^2} \tag{6.2.1}$$

Similarly for Wigner (GOE) the $P(r)$ is given by Wigner-like surmise [108],

$$P_W(r) = \frac{27}{8}\,\frac{r+r^2}{(1+r+r^2)^{5/2}} \tag{6.2.2}$$

Here, one should be clear that for the nearest neighbour spacing distribution method, the minimal matrix size will be of 3×3 unlike the NNSDs where one can start with a 2×2 matrix. The reason behind this is very simple, in NNSD we only deal with the spacing between nearest levels, but in $P(r)$ distribution we take the ratio of the spacings of consecutive levels which is possible only if we have at least three states.

Moreover, along with the theoretical distributions specified in Eq. (6.2.1) and

Eq. (6.2.2) it is also suggested in [108] that the difference $\delta P(r) = P(r) - P_W(r)$ between numerics and the Wigner surmise (6.2.2) can be approximated by the following expression,

$$\delta P(r) = \frac{C}{(1+r)^2}\left[\left(r+\frac{1}{r}\right)^{-1} - 2\,\frac{\pi-2}{4-\pi}\left(r+\frac{1}{r}\right)^{-2}\right] \tag{6.2.3}$$

where the parameter C is obtained by fitting the expression $P(r) = P_W(r) + \delta P(r)$.

In addition to r_n, Oganesyan and Huse [101] considered the distribution of the ratios $\tilde{r}_n$ defined by

$$\tilde{r}_n = \frac{min(s_n, s_{n-1})}{max(s_n, s_{n-1})} \tag{6.2.4}$$

Moreover, as stated in [108], for a given $P(r)$ one can always calculate $P(\tilde{r})$. We here deal with the average values of r and $\tilde{r}$ represented by $\langle r\rangle$ and $\langle\tilde{r}\rangle$ respectively. The theoretical values of $\langle r\rangle$ for the GOE part is 1.75 and for the Poisson part is infinity (∞), whereas if $\langle\tilde{r}\rangle$ is considered then the theoretical value for GOE goes down to 0.536 and for Poisson is 0.386. Hence we use the $P(r)dr$ analysis for the study of spacing of energy levels that are nearest neighbor of each other for different many body systems. Further, we shall introduce the interpolating matrix ensemble.

6.3 Introducing an interpolating random 3×3 matrix ensemble and mapping to a matrix of order $d \times d$

We shall start with a 3×3 matrix ensemble, with an interpolating parameter called λ. We can denote its Hamiltonian as $H_{3\times3}$ and can be represented as under [109],

$$H_{3\times3} = \begin{bmatrix} A & B & C \\ B & D & E \\ C & E & F \end{bmatrix} = \begin{bmatrix} -pvx & 0 & 0 \\ 0 & 0 & 0 \\ 0 & 0 & pvx \end{bmatrix} + \lambda \begin{bmatrix} a & b & c \\ b & d & e \\ c & e & f \end{bmatrix} \tag{6.3.1}$$

Here in Eq. (6.3.1), x and y are the independent Poisson variables with average unity so that the joint probability distribution $P(x, y)$ where $0 \leq x, y \leq \infty$ is as follows:

$$P(x, y)dxdy = e^{-(x+y)} \tag{6.3.2}$$

Secondly, the variables like a,b,c,d,e and f are independent Gaussian variables with zero center. Precisely, we can say that a, d and f are independent $G(0, 2v^2)$ variables with variance equal to $2v^2$, whereas b, c and e are independent $G(0, v^2)$ variables with variance equal to v^2. Also here p is a constant introduced, analogous to the work done in [110] where the Poisson to GOE transition is observed for a 2×2 ensemble using NNSD. The importance of p is understood from Eq. (6.3.5) in identifying the role of the mean spacing of the unperturbed spectrum. When $\lambda = 0$, $H_{3\times3}$ gives the Poisson result for $P(r)$ as represented by Eq. (6.2.1). Similarly as $\lambda \to \infty$, $H_{3\times3}$ approaches to GOE as stated in Eq. (6.2.2). Thus, as λ changes from 0 to ∞, $H_{3\times3}$ generates Poisson to GOE transition in the $P(r)$ and related averages. In Fig. (6.1), we have constructed a plot for $H_{3\times3}$ Hamiltonian, the related averages of $P(r)$ i.e. $\langle r \rangle$ and $\langle \tilde{r} \rangle$ have been plotted as a function of λ. For $\langle r \rangle$, one can easily observe a transition from Poisson ($\langle r \rangle \sim \infty$) to GOE ($\langle r \rangle = 1.75$) as the value of λ increases gradually from $\lambda = 0$ to $\lambda = 1$. Moreover, it can be easily seen that for $\lambda = 0$, the average spacing between the nearest eigenvalues is $\overline{D}_0 = pv$. Now, the joint probability distribution, $\rho(A, B, C, D, E, F)$, for the matrix elements A, B, C, D, E and F of $H_{3\times3}$ is easy to write down. If we denote the eigenvalues of $H_{3\times3}$ as $e_i (i = 1,\ 2 \text{ and } 3)$ and the orthogonal matrix that diagonalizes $H_{3\times3}$ is generated by three angles and say they are $\theta_i (i = 1,\ 2 \text{ and } 3)$. Then, the joint probability distribution is given by,

$$\rho(A, B, C, D, E, F) = \mathcal{N} exp - \left\{ \frac{(A + pvx)^2 + D^2 + (F - pvy)^2}{4\lambda^2 v^2} + \frac{B^2 + C^2 + E^2}{\lambda^2 v^2} \right\} \tag{6.3.3}$$

and $dAdBdCdDdEdF$ is of the form $\prod_{i<j} |e_i - e_j| f(\theta_1\theta_2\theta_3) de_1 de_2 de_3 d\theta_1 d\theta_2 d\theta_3$. It is to be noted that $\mathcal{N}$ is a normalization constant and the function $f(\theta_1\theta_2\theta_3)$ follows from the Jacobi transformation from (A, B, C, D, E, F)to $(e_1, e_2, e_3, \theta_1, \theta_2, \theta_3)$. Putting $e_i = 2\lambda v x_i$ we have,

$$\rho(x_1, x_2, x_3, \theta_1, \theta_2, \theta_3) dx_1 dx_2 dx_3 d\theta_1 d\theta_2 d\theta_3 =$$

$$\mathcal{N}' exp - \left\{ \frac{p^2 v^2}{4\lambda^2 v^2}(x^2 + y^2) + \frac{pv}{\lambda v}[x f_1(x_1, x_2, x_3, \theta_1, \theta_2, \theta_3) - y g_1(x_1, x_2, x_3, \theta_1, \theta_2, \theta_3)] \right\}$$

$$\times \prod_{i<j} |x_i - x_j| f(\theta_1, \theta_2, \theta_3) dx_1 dx_2 dx_3 d\theta_1 d\theta_2 d\theta_3 \tag{6.3.4}$$

From the above Eq. (6.3.4) one can observe that, f_1 and g_1 transform A and F in Eq.(6.3.1)into x_i(i.e. e_i) and θ_i, whereas $\mathcal{N}'$ is the normalization constant. Further, integrating the R.H.S. of Eq.(6.3.4) over $(\theta_1\theta_2\theta_3)$ and also over x and y with the weight factor $P(x, y) = exp(x + y)$ will give $\rho(x_1, x_2, x_3)$ and there by $P(r)$. Thus we can infer that Eq.(6.3.4) gives the important result that $\rho(e_1, e_2, e_3)$ and therefore the $P(r)$ will depend only the transition parameter Λ. This transition parameter Λ can be expressed as under:

$$\Lambda = \frac{\lambda^2 v^2}{p^2 v^2} = \frac{\lambda^2 v^2}{[\overline{D_0}]^2} \tag{6.3.5}$$

On observing it carefully, it is seen that the value of Λ is nothing but the square of the admixing matrix element divided by the average spacing between the unperturbed $(\lambda = 0)$ levels. In the next section, we shall introduce a general $d \times d$ matrix for the study of Poisson to GOE transition and also show that this ensemble can be mapped to the $H_{3\times3}$ ensemble.

6.3.1 A general $d \times d$ ensemble : Observing the Poisson to GOE transition

Following the work in [111], we will consider the interpolating Hamiltonian ensemble

$$H_\lambda = \frac{H_0 + \lambda V}{1 + \lambda^2} \tag{6.3.6}$$

where H_0 is a diagonal matrix with $(H_0)_{ii}$, $i = 1, 2, ..., d$, being independent $G(0, 1)$ variables. Similarly V is chosen as a GOE with matrix elements variance v^2 (and again

for diagonal matrix elements it is $2v^2$). For H_0, the value of spectral variance comes out to be $\overline{\sigma^2(H_0)} = 1$ and the one generated by V is $\overline{\sigma^2(V)} = v^2(d+1)$. We choose H_0 and V such that $\overline{\sigma^2(H_0)} = \overline{\sigma^2(V)}$ giving $v^2 \sim 1/d$ for large d. In the same manner, as we have $\sigma(H_0) = 1$, we have $D_0 \sim (d\rho_0)^1$. Here, ρ_0 is the eigenvalue density that is generated by H_0. Hence the transition parameter for the H ensemble given by Eq.(6.3.6)is $\Lambda = \frac{\lambda^2 v^2}{[D_0]^2}$. In this expression, if we replace ρ_0 by its average value then we have the final value of the transition parameter Λ as,

$$\Lambda = \frac{\lambda^2 d}{2\pi} \tag{6.3.7}$$

In this work, large scale numerical investigations have been carried out with different matrix dimensions (d) like 100, 300, 500, 800 and 1000, as here we do not have an analytical solution for $P(r)$ for the H_λ ensemble. Also, here we do not study the $P(r)dr$ as a function of the interaction strength λ, but instead the nature of related averages $\langle r \rangle$ and $\langle \tilde{r} \rangle$ versus λ. Fig. (6.2) (upper panel) and (lower panel) gives the behavior of $\langle r \rangle$ and $\langle \tilde{r} \rangle$ versus λ respectively. We represent different matrix dimension by different colors and pattern for better understanding. For Fig. (6.2) (upper panel), it can be observed that as the matrix dimension increases the transition is more faster which can be compared from the nature of $d = 100$ and $d = 1000$. The transition for $d = 100$ occurs near $\langle r \rangle \sim 3.6$ whereas for the higher dimension $d = 1000$ it is near $\langle r \rangle \sim 2.25$. In the same manner, for panel (lower panel) in Fig. (6.2) we can see that transition of $\langle \tilde{r} \rangle$ is faster for $d = 1000$ near $\langle \tilde{r} \rangle \sim 0.43$ and for $d = 100$ it is $\langle \tilde{r} \rangle \sim 0.4$. We can conclude from the results that the values of related averages $\langle r \rangle$ and $\langle \tilde{r} \rangle$ depend on the matrix dimension d and the transition from Poisson to GOE is faster as the value of d increases. Thus, one can say that the curves of $\langle r \rangle$ and $\langle \tilde{r} \rangle$ are not universal when plotted against the λ parameter. But then, if the dimension d goes to infinity, one might expect that even an infinitesimal λ would take the system to the chaotic domain. This sudden transition with $\lambda > 0$ is similar to the situation with Poisson to GOE or GUE [30, 112] and GOE to GUE [113] transitions. Also, for physical systems the matrix dimension d is ill defined. Hence, the results discussed

above cannot be considerably true as they are not universal and the d-dependence totally dominates over the contribution from the parameter λ. The solution to this problem is to derive the $P(r)$ as a function of both, λ and d and then one can identify (as done in [30, 112, 113]). Hence we introduce the transition parameter defined above Λ, that depends upon (λ, d) as per given in Eq. (6.3.5). Now we calculate the related averages and their behavior with respect to Λ for different matrix dimensions. The results are shown in Fig. (6.3 a) for $\langle r \rangle$ and Fig. (6.3 b) representing for $\langle \tilde{r} \rangle$, versus Λ. It is to be noted here that as soon as we define the new transition parameter Λ in terms of λ and d, the results of related averages become independent of the matrix dimensions (d). In other words we say that the transition from Poisson to GOE is uncorrelated with the d value. This condition is called the Universality which is a significant condition in itself. Another thing that should be marked here is that the transition observed here is slow. Previously such a behavior was also observed in [30]. The continuous curves in Figs. (6.3)(upper panel) and (lower panel) are due to fitting exponential decay and exponential growth functions of order 3 with the numerical results respectively.

Now, for any transition that occurs in a system, one may always expect a transition point where the curve changes its nature or the type of distribution. In the present system also it is possible to define a critical value Λ_c for the transition parameter Λ for the Poisson to GOE transition that defines the onset of GOE fluctuations. From Fig. (6.3), the transition curves of $\langle r \rangle$ and $\langle \tilde{r} \rangle$ do not display phase transition as a function of Λ and hence we define the critical value of the transition parameter using a meaningful criterion. We here fix the critical value 'Λ_c' at 80% change in the $\langle \tilde{r} \rangle$ value, which comes out to be 0.5 as the transition is from $\langle \tilde{r} \rangle = 0.386$ (Poisson) to $\langle \tilde{r} \rangle = 0.536$ (GOE). This can be verified from the Fig.(6.3) and also the corresponding value of Λ_c comes out to be $\Lambda_c = 0.3$. For this value of Λ_c we get the corresponding value of $\langle r \rangle$ from Fig. (6.3 a) to be $\langle r \rangle = 2$. Thus, one can use this criterion to measure the onset of chaos in complex many body systems which will be discussed further in the next section. But before that we shall check the mapping between 3×3

and $d \times d$ matrix ensembles that are discussed so far.

6.3.2 Mapping 3×3 and $d \times d$ matrix

Here we shall check the mapping between 3×3 matrix ensemble defined in Eq. (6.3.1) and $d \times d$ matrix given in Eq. (6.3.6). In order to avoid confusion between the λ used in the expressions of both the ensembles, we denote the λ used in $H_{3\times3}$ as $\lambda_{3\times3}$ from now onwards. For the 3×3 matrix ensemble defined in Eq. (6.3.1) the behavior of related averages $\langle r \rangle$ and $\langle \tilde{r} \rangle$ versus $\lambda_{3\times3}$ is studied using 50000 members. Using these and the results in Fig. (6.3), one can determine the value of Λ ($\sim \lambda d^{1/2}$) for a given value of $\lambda_{3\times3}$ that gives the same value for $\langle r \rangle$ and similarly for $\langle \tilde{r} \rangle$. Hence, using $\langle r \rangle$ we construct a plot of $log\lambda_{3\times3}$ versus $log\lambda d^{1/2}$ (which is $\sim \Lambda^{1/2}$) shown in Fig. (6.4 (upper panel)) and in the same manner a plot is constructed for $log\lambda_{3\times3}$ versus $log\lambda d^{1/2}$ using $\langle \tilde{r} \rangle$ shown in Fig. (6.4 (lower panel)). In both the plots, matrix dimensions ranging from $d = 300$, 500, 800 and 1000 are taken and it can be observed that there is a linear correlation between the curves of $ln\lambda_{3\times3}$ and $ln\Lambda^{1/2}$, irrespective of the value of matrix dimension (d). The straight lines are due to a linear fit to the results of $ln\lambda_{3\times3}$ versus $ln\Lambda^{1/2}$ obtained from $\langle r \rangle$ and $\langle \tilde{r} \rangle$. Moreover, it is interesting to check that both the results give similar slope. This indicates that the mapping between 3×3 and $d \times d$ ensembles is same for both $\langle r \rangle$ and $\langle \tilde{r} \rangle$. Therefore the $\langle r \rangle$ versus Λ and $\langle \tilde{r} \rangle$ versus Λ transition curves can be derived by solving the 3×3 ensemble defined by Eq.(6.3.1)and this will be discussed in near future.

6.3.3 $P(r)dr$ analysis for random matrix ensembles

1. **BEGOE(1+2)-F**

   For the BEGOE(1+2)-F random matrix ensemble of bosons with a fictitious F spin studied in Chapter 3, the $P(r)dr$ analysis is done and we also observe a transition from regularity to chaoticity as the strength of the two body λ

increases. Such a transition has not been studied yet using the ratio of consecutive level spacings. For the configuration chosen for this system i.e. for $m = 10$ bosons and $\Omega = 4$ single particle states, we have in Fig. (6.5) the trend of $P(r)$ plotted for two spins $F = 2$ and $F = 5$ with their dimensionalities being 750 and 286 respectively. This is carried out using 50 members. It is clearly seen that the nature of $P(r)$, say for $F = 2$ is Poisson (blue curve) when $\lambda = 0.008$ and slowly it moves to GOE (red curve) as the value of λ approaches to 0.5. Similar is the behavior observed for spin $F = 5$ where the Poisson nature is observed at $\lambda = 0.002$ and it is transformed to GOE as λ reaches 0.5.

2. **BEGOE(1+2)-$S1$**

   The BEGOE(1+2)-F random matrix ensemble of spin one bosons discussed in Chapter 4 also exhibits the Poisson to GOE transition observed by NNSD. We shall again verify this by the $P(r)dr$ method. For this model we had chosen $m = 8$ bosons distributed in $\Omega = 4$ single particle states. The probability distribution $P(r)dr$ has been plotted for different values of two body interaction strength λ as shown in Fig. (6.6) for 100 members. There are total $S = 0,1,2,...8$ spin values possible in this system out of which we shall show only for spin $S = 0$ and $S = 8$ (extremities) whose dimensionalities are $d = 714$ and $d = 165$ respectively. It is clearly seen from the Fig. (6.6) that the behavior of $P(r)$, say for $S = 0$ is Poisson (blue curve) when $\lambda = 0.015$ and slowly it moves to GOE (red curve) as the value of λ approaches to 0.032. Similar is the behavior observed for spin $S = 8$ where the Poisson nature is observed at $\lambda = 0.017$ and it is transformed to GOE as λ reaches 0.033.

It is certainly clear up to this stage that the method of $P(r)dr$ is fairly applicable to the random matrix ensembles of bosonic and fermionic systems where one observes the crossover from regularity to chaoticity. Further, we shall extend our investigation on $P(r)dr$ for some realistic finite lattice systems of interacting spins half where one does not require contribution from random numbers. This is discussed in the next section for 1D finite lattice chains of

interacting spins.

6.4 One dimensional finite lattice chain of interacting spins$-1/2$: A brief introduction

Interaction between spins is an emerging area of research these days, especially when one deals with quantum phase transitions, localization in disordered systems, quantum computing, superconductivity, quantum entanglement, etc [114]. There are also been attempts to simulate spin-1/2 chains with cold gases in the optical lattices [115]. The lattice chains of interacting spins-1/2 are prototype quantum many body systems where the exchange interaction between particles of spin-1/2 is usually described by the Heisenberg models. This is again one of the most important models of magnetism and has been investigated for decades [114, 116, 117, 118]. An exact analytical solution to the one-dimensional (1D) spin-1/2 Heisenberg model was proposed by Bethe in 1931 [119, 120] and this became very helpful in studying those quantum many body systems which are exactly solvable. For these lattice chains, chaos is studied on the basis of position or strength of the defect site which is discussed ahead. A transition from integrability to chaos was observed for such systems using the nearest neighbor spacing distribution (NNSD) in past. But no such analysis is done so far using the $P(r)$ distribution explained above.

In the present work, we choose two different Heisenberg's lattice chains and observe a transition from Poisson to GOE by using the theory of $P(r)$ distribution explained above. The section briefs about these finite lattice chains of interacting spins half, whereas the mathematical part including the construction of the Hamiltonian is detailed in the Appendix C part at the end. To start with, one can encounter these chains with a static magnetic field which is responsible of the Zeeman splitting in the energy levels. These systems can be viewed as finite

isolated lattice chains where each lattice site is assigned with a spin (spin-1/2 here) pointing upwards or downwards. Let L be the total number of lattice sites in a chain. Due to a static magnetic field in say z-direction, every spin experiences a Zeeman splitting of the order ω. But at one particular site, the energy splitting is different from the rest given as $\omega + \varepsilon$ due to magnetic field slightly larger at that point [109]. This is the onset of chaos and is referred to as 'defect'- a situation which arises at a particular lattice point due to a slightly high magnetic field at that point. It is the position of this defect site or the value of defect strength (ε defined above) which decides the chaotic behavior of the chain. The chain is said to be integrable or rather 'clean' when it is devoid of such a defect, and such a system can be solved with the Bethe ansatz [119]. Moreover, if the defect site is located at the end points of an open chain, the chain is still clean [121]. However, if this defect site is located at the middle of chain with a considerable defect strength (ε) then the system becomes chaotic. The spacing statistics then follow the Wigner surmise defined by the NNSD previously. For the present investigation, this transition from Poisson to GOE is studied for two Heisenberg's models but by using $P(r)$ distribution. Moreover, the interaction between spins here is considered for nearest neighbors only. The up-spin here denotes an excitation which is to be propagated throughout the chain. Also, for the lattice chain described in the present investigation z component of the total spin $\sum_{n=1}^{L} S_n^z$ is conserved, so the states with same number of excitations are coupled. To avoid degeneracy found in the spectrum of a closed chain(with periodic boundary conditions) we here consider open chains so that an excitation at site 1 moves up to the $(L-1)$ site and the momentum is not conserved. Chaos in these systems arise because of the defect site within the system, its position and its strength. These lattice chains of interacting spins half can be classified on the basis of different Heisenberg models (XXX, XXZ, XYZ). In this chapter we will be analyzing lattice chains that reflect the XXX (isotropic) model and XXZ (anisotropic) model.

6.4.1 Analyzing the Poisson to GOE transition

(a) **Isotropic chain : XXX Heisenberg model**

This is an isotropic version of the Heisenberg model. The Hamiltonian here is described by the equation (C-3) of Appendix C. For this model, all the components of the interaction term have the same strength i.e. $J = J_x = J_y = J_z$ and hence called isotropic. We have with us finite one dimensional lattice chain with $L = 14$ number of lattice sites. As discussed above, the number of excitations are denoted by up-spins and let they be $L/2$ i.e. total 7 excitations and the rest sites posses down-spins. For such a system, the dimensionality of Hamiltonian matrix will be 3432, calculated by the expression of dimensionality (C-4) as stated in Appendix C. Till now the system is devoid of any kind of defect and hence called clean. But to study the Poisson to GOE transition, a defect is introduced at the middle of the chain. Then the defect site would be $L/2 = 7$ and then $P(r)$ is evolved by varying the defect strength ε for $\varepsilon < 0 \leq J$. Value of the interaction strength J is set as 1 here. The results in Fig. 6.7 show that for $\varepsilon = 0$ the $P(r)$ gives a Poisson curve and as we gradually increase the value of ε to 1, a clear transition to GOE is observed. Also here the related averages are calculated with respect to the defect strength and plot is constructed in Fig. 6.8. In the first panel of Fig. 6.8, one can observe that for $\varepsilon = 0$ the value of $\langle r \rangle$ is equal to ∞ (Poisson) and as ε approaches to 1 ($\varepsilon \sim J$) we achieve the theoretical limit indicating chaos (GOE) at $\langle r \rangle = 1.75$. Similarly in the second panel of Fig. 6.8, a Poisson nature is observed at $\langle \tilde{r} \rangle = 0.386$ for $\varepsilon = 0$ and a complete chaos is introduced at $\langle \tilde{r} \rangle = 0.536$ for $\varepsilon = 1$. Demarcation between the Poisson and GOE region giving the critical value of the defect strength at which there is a clear onset of chaos, is found to be $\varepsilon_c = \varepsilon(\langle \tilde{r} \rangle = 0.5)$. The corresponding value of $\varepsilon_c = 0.1$. Thus one can understand that as the strength of the defect in the middle of an isotropic chain increases considerably the system

approaches to chaos.

(b) **Anisotropic chain : XXZ Heisenberg model**

Introduced now is the Heisenberg's XXZ model which is an anisotropic model. The construction of Hamiltonian here is only a step different from the previously studied isotropic XXX model and is elaborated in the Appendix C. In this case, the three components of the interaction strength J are not equal but they are in a relation $J_x = J_y \neq J_z$ (J_x and J_y are commonly denoted as J_{xy}). We consider a finite lattice chain of $L = 18$ lattice sites. Moreover, we modify the criterion of choosing the number of excitation according to [71] and choose subspaces filled with $L/3$ up-spins which takes care of the condition $S^z \neq 0$. Thus we have $L/3 = 6$ number of excitations to be distributed on $L = 18$ lattice sites, and the dimensionality is given by the expression (C-6) in Appendix C and this comes out to be 18564. As done in the former case, here also the defect is introduced at the middle of the chain $L/2$ (i.e. on the 9th site)and the $P(r)$ is calculated for different values of defect strength ε where $\varepsilon < 0 \leq 1$. The value of the flip-flop strength (J_{xy}) is set as 1, and the strength of the Ising term (J_z) is set as 0.5. The $P(r)dr$ analysis is shown in Fig. (6.9), where one can observe a Poisson curve for $\varepsilon = 0.001$ and then as the value of ε increases to 0.3 the system becomes chaotic. A clear crossover from regular to chaos is thus observed. Also we calculate the related averages with respect to the defect strength shown in Fig. (6.10). From the plot of $\langle r \rangle$ versus ε one observes that for $\varepsilon = 0$ the value of nature of $\langle r \rangle$ is Poisson and a rapid transition to GOE nature is observed as the value of for ε approaches to 1. This region exhibits chaos and it fairly matches with the theoretical value $\langle r \rangle = 1.75$. In the same manner, the nature of $\langle \tilde{r} \rangle$ is also plotted with respect to ε and the numerical results are in good agreement with the theoretical results. For $\varepsilon = 0$, the value of $\langle \tilde{r} \rangle = 0.386$ which represents a Poisson behavior. And then, for ε leading to 1 we can very well observe

the a chaotic behavior where the value of $\langle \tilde{r} \rangle$ is equal to 0.536.

6.5 Conclusions

The central theme of this chapter is to study the transition from regular domain (Poisson) to chaotic domain (GOE) by using the method of ratio of consecutive level spacings $[P(r)dr]$. Introduced here is an interpolating matrix ensemble with a parameter λ giving Poisson ($\lambda = 0$) to GOE ($\lambda \to \infty$) transition. $P(r)dr$ is studied for this ensemble using different matrix dimensions ($d \leq 1000$). It is observed from the results of related averages that the transition from Poisson to GOE is faster as the value of dimensionality (d) increases. But this dependence on dimension is something which cannot be called as Universal. Thereby, a new transition parameter $\Lambda \sim \lambda^2 d$ is introduced and we find that the curves achieve a universal form independent of the matrix dimension. We verify this by the results of mapping between the 3×3 and $d \times d$ matrices and the results are satisfactory. Moreover, we also construct $P(r)dr$ for the BEGOE(1+2)-$S1$ and BEGOE(1+2)-F models studied in earlier chapters. Lastly, we introduce one-dimensional (1D) finite interacting spin-1/2 lattice chains using Heisenberg's XXX and XXZ models. Here too we observe a transition from Poisson to GOE as the strength of defect ε is increased.

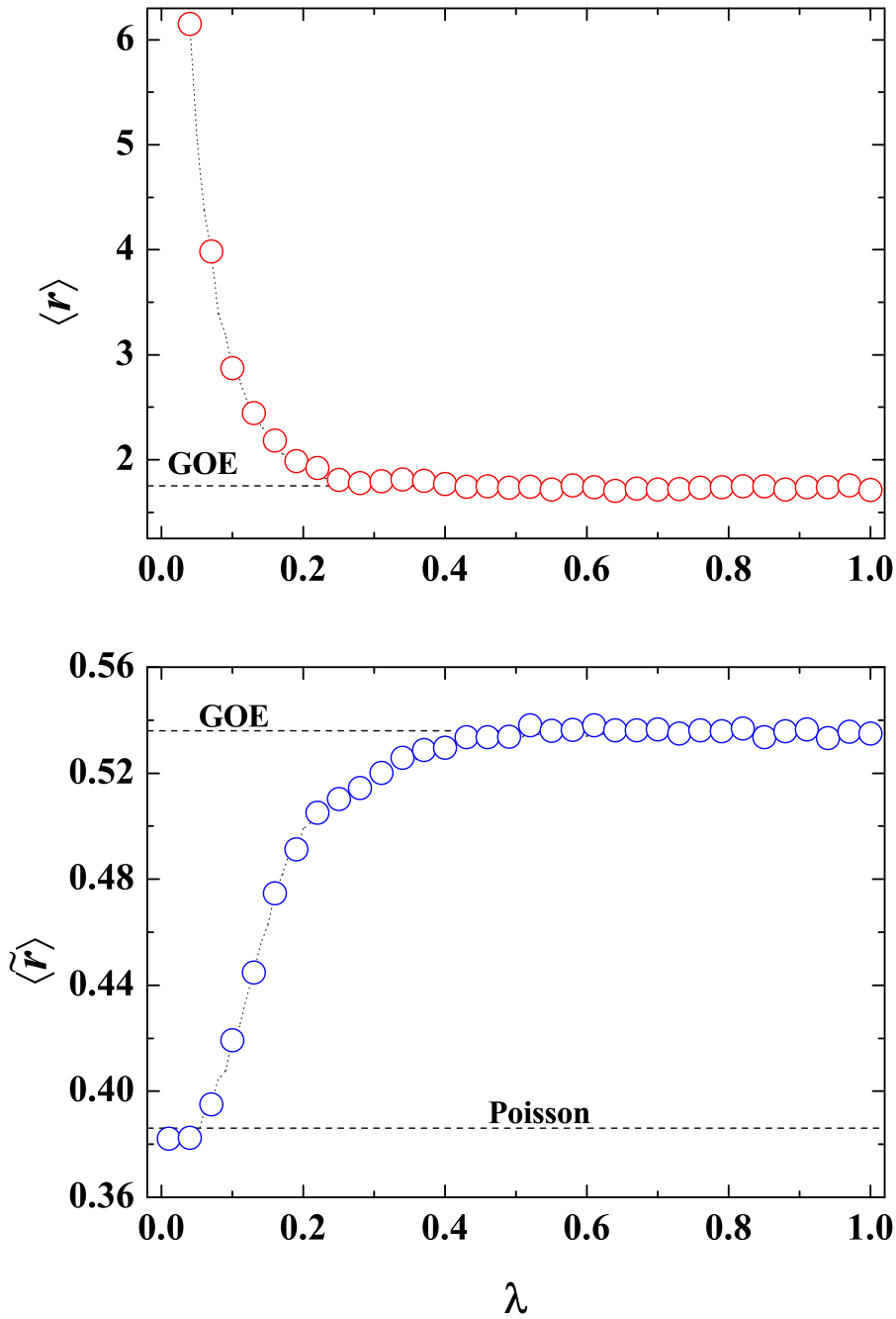

Figure 6.1: For the $H_{3\times3}$ Hamiltonian, the related averages of $P(r)$ are plotted. The first panel shows the nature of $\langle r\rangle$ versus λ and the lower panel shows for $\langle\tilde{r}\rangle$ versus λ. One can easily observe that as the value of λ increases, $\langle r\rangle$ makes a transition from Poisson ($\langle r\rangle \sim \infty$) to GOE ($\langle r\rangle = 1.75$) and similarly $\langle\tilde{r}\rangle$ experiences a transition to GOE $\langle\tilde{r}\rangle = 0.536$ as the λ increases gradually.

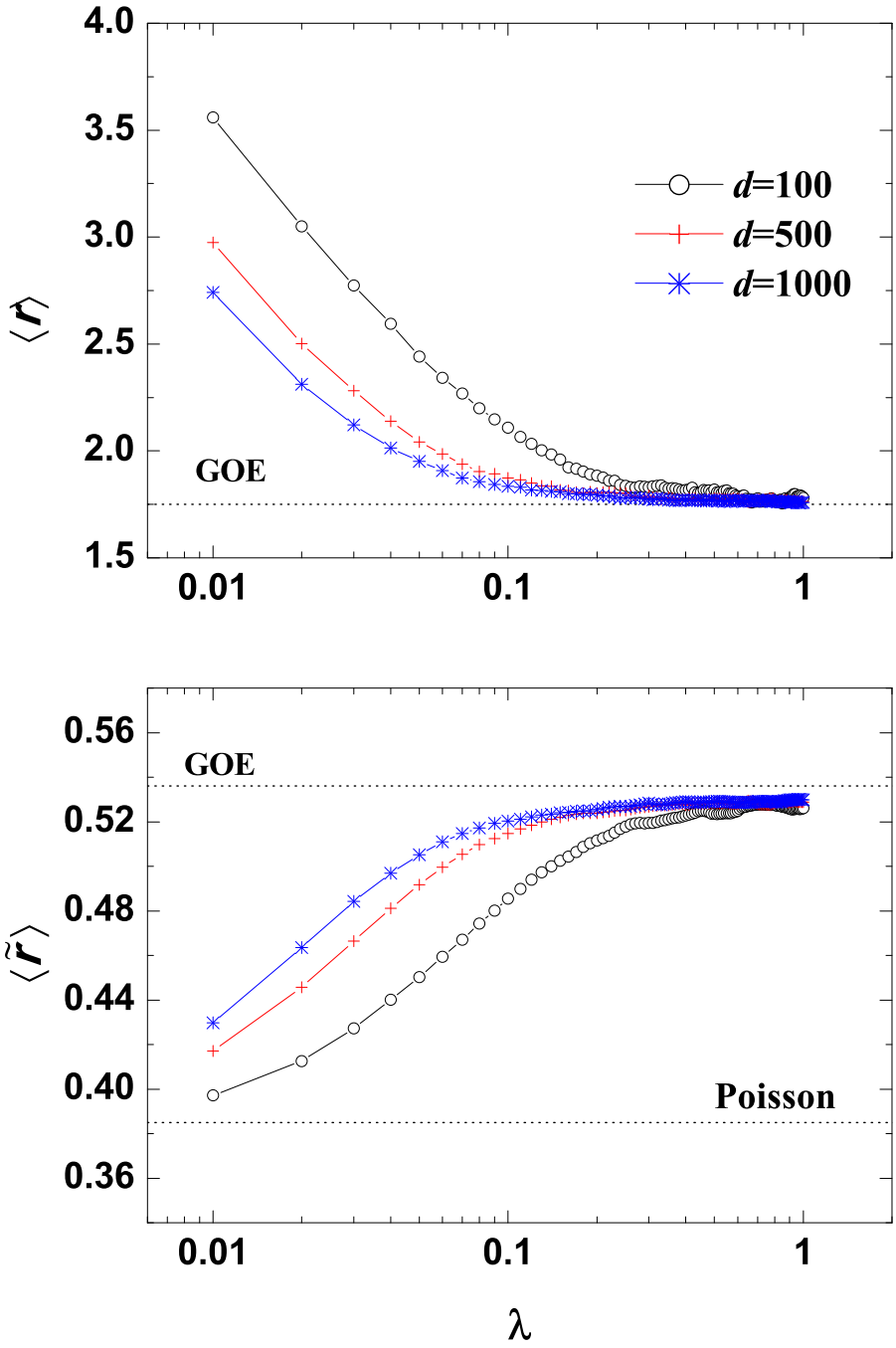

Figure 6.2: Variation of $\langle r \rangle$ (upper panel) and $\langle \tilde{r} \rangle$ (lower panel) as a function of λ for $d \times d$ matrix ensembles. Results are shown for matrix dimension d going from 100 to 1000. In each calculation, en ensemble of 1000 members is used.

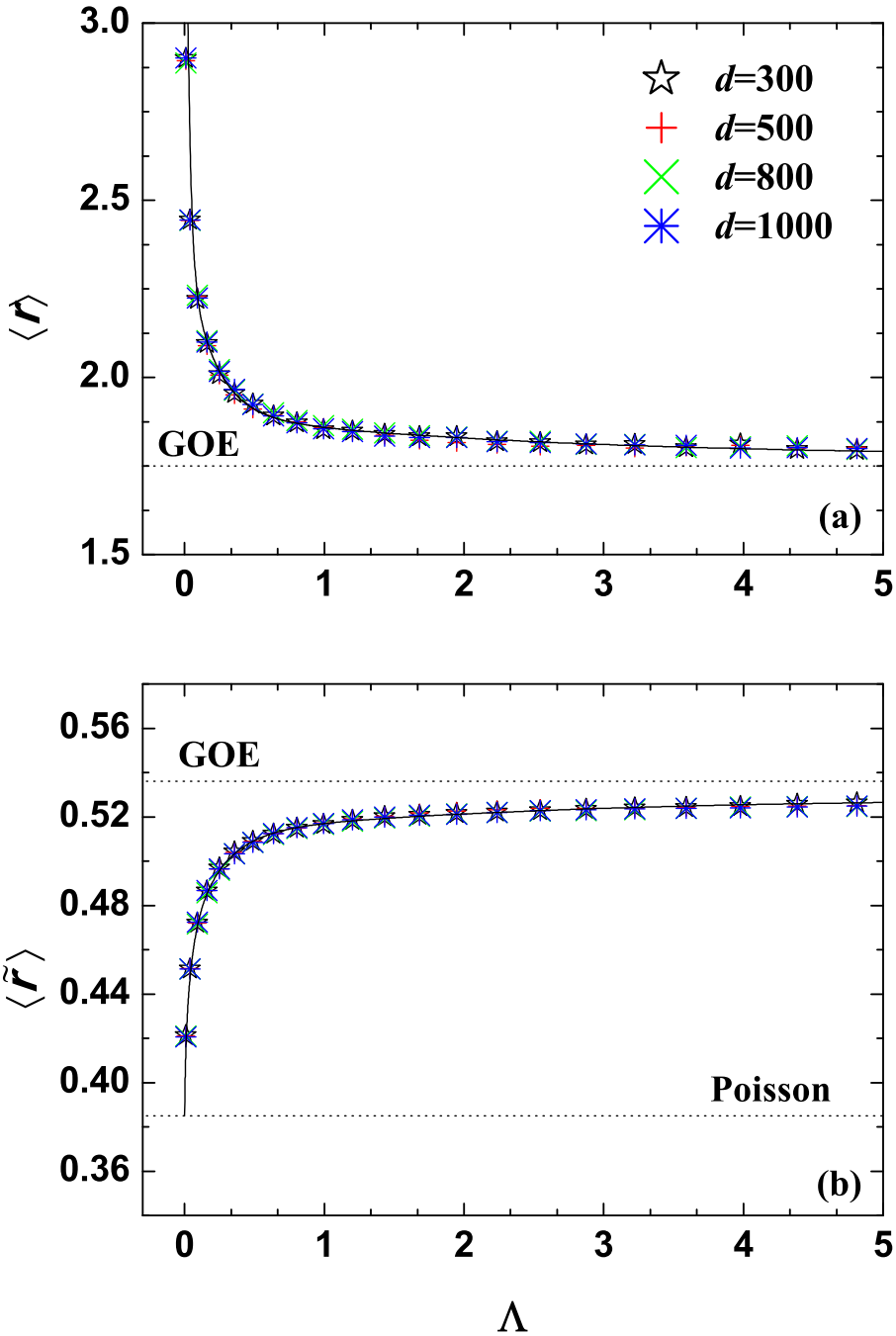

Figure 6.3: Variation of $\langle r \rangle$ (upper panel) and $\langle \tilde{r} \rangle$ (lower panel) as a function of Λ for $d \times d$ matrix ensembles. Results are shown for matrix dimension d going from 300 to 1000. In each calculation, en ensemble of 1000 members is used. The continuous curves represent the best fit to the results giving the universal transition curves.

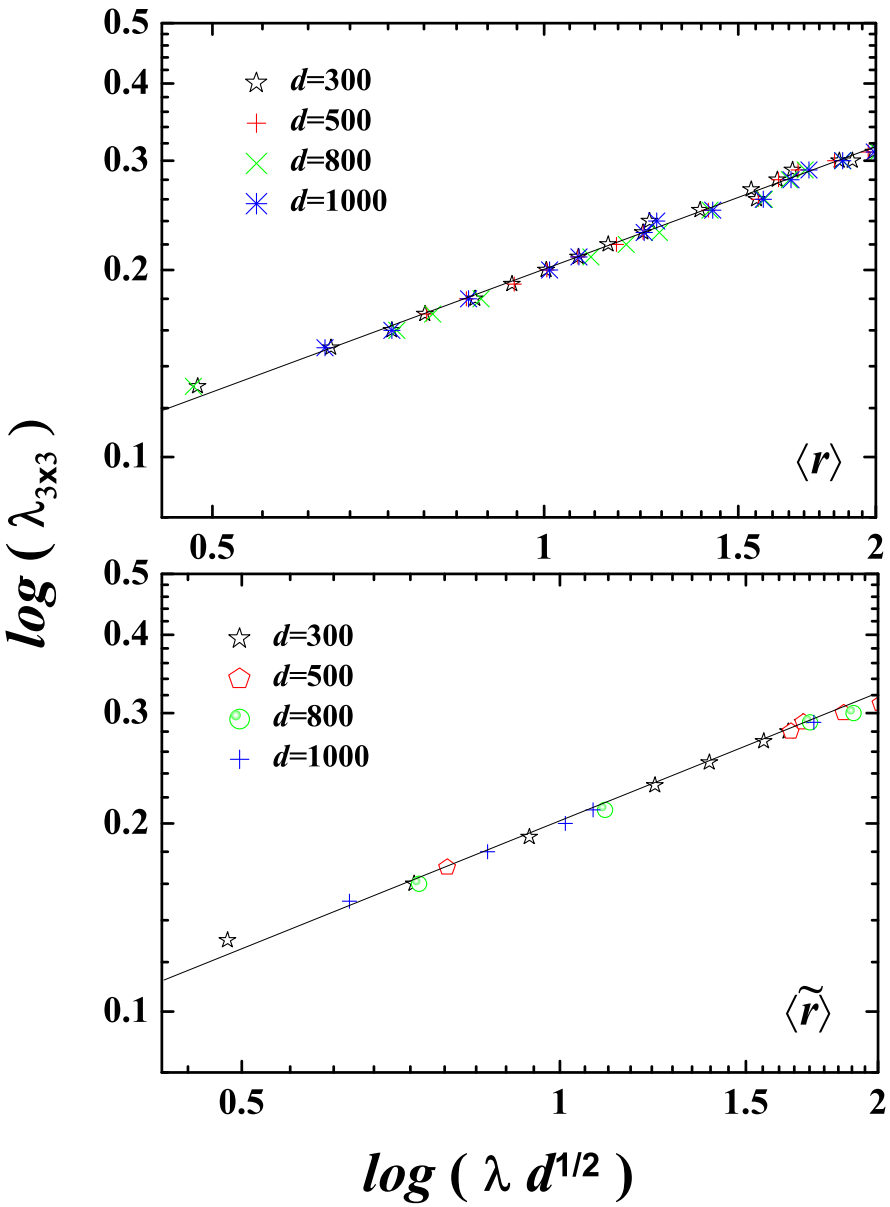

Figure 6.4: $log(\lambda_{3\times3})$ from 3×3 ensemble versus $log(\lambda d^{1/2})$ (which is$\sim \Lambda^{1/2}$) for various matrix dimensions d. Upper panel gives the result obtained from $\langle r \rangle$ and the lower panel from $\langle \tilde{r} \rangle$. The straight lines are obtained via fitting linear relation to numerical results.

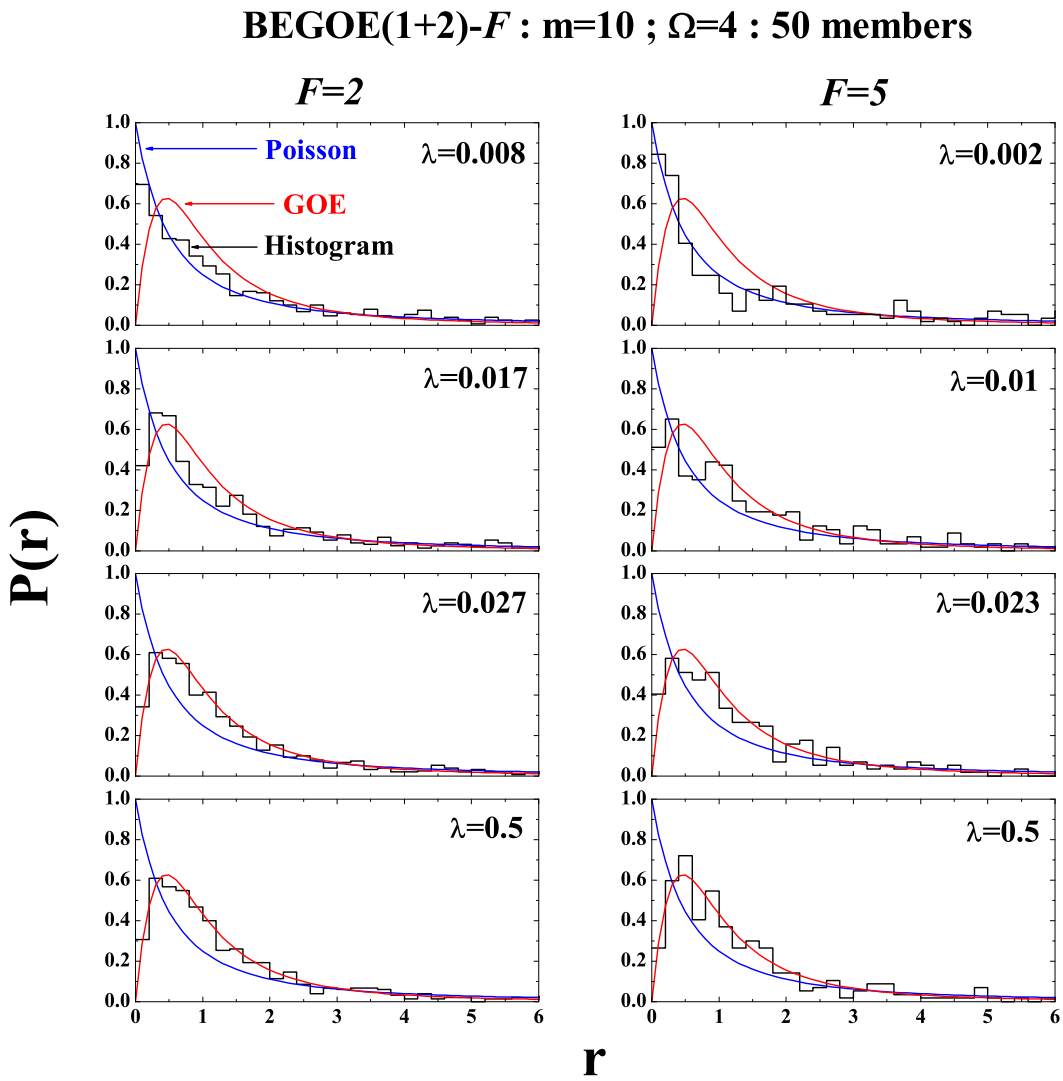

Figure 6.5: For BEGOE(1+2)-F, the plot of $P(r)$ versus r shows the histograms representing the numerical results and they are compared with the theoretical curves of Poisson and Wigner(GOE). A clear transition is observed from Poisson to GOE as the value of λ increases. Here we have shown for spins $F = 2$ and $F = 5$ using 50 members

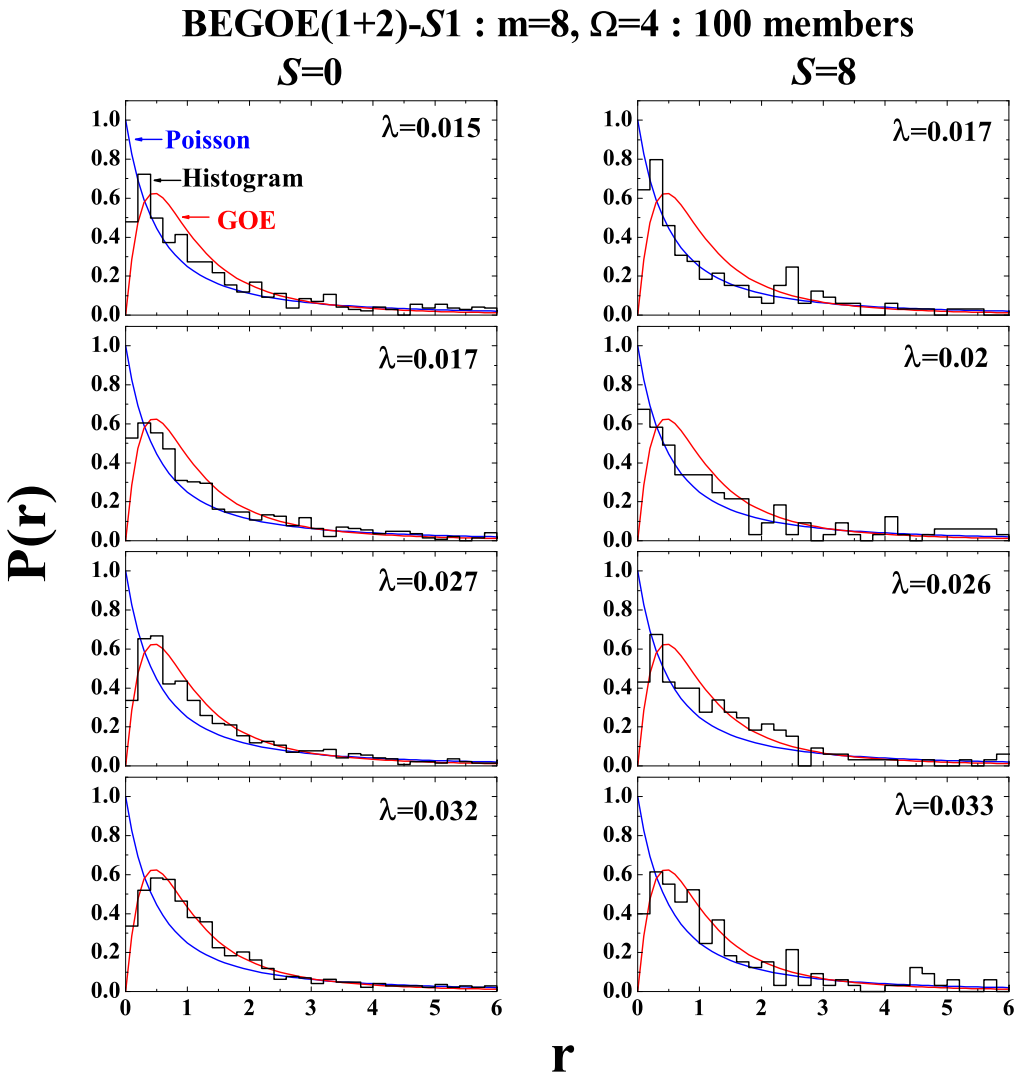

Figure 6.6: For BEGOE(1+2)-$S1$, the plot of $P(r)$ versus r shows the histograms representing the numerical results and they are compared with the theoretical curves of Poisson and Wigner(GOE). A clear transition is observed from Poisson to GOE as the value of λ increases. We have shown for spins $S = 0$ and $S = 8$ using 100 members

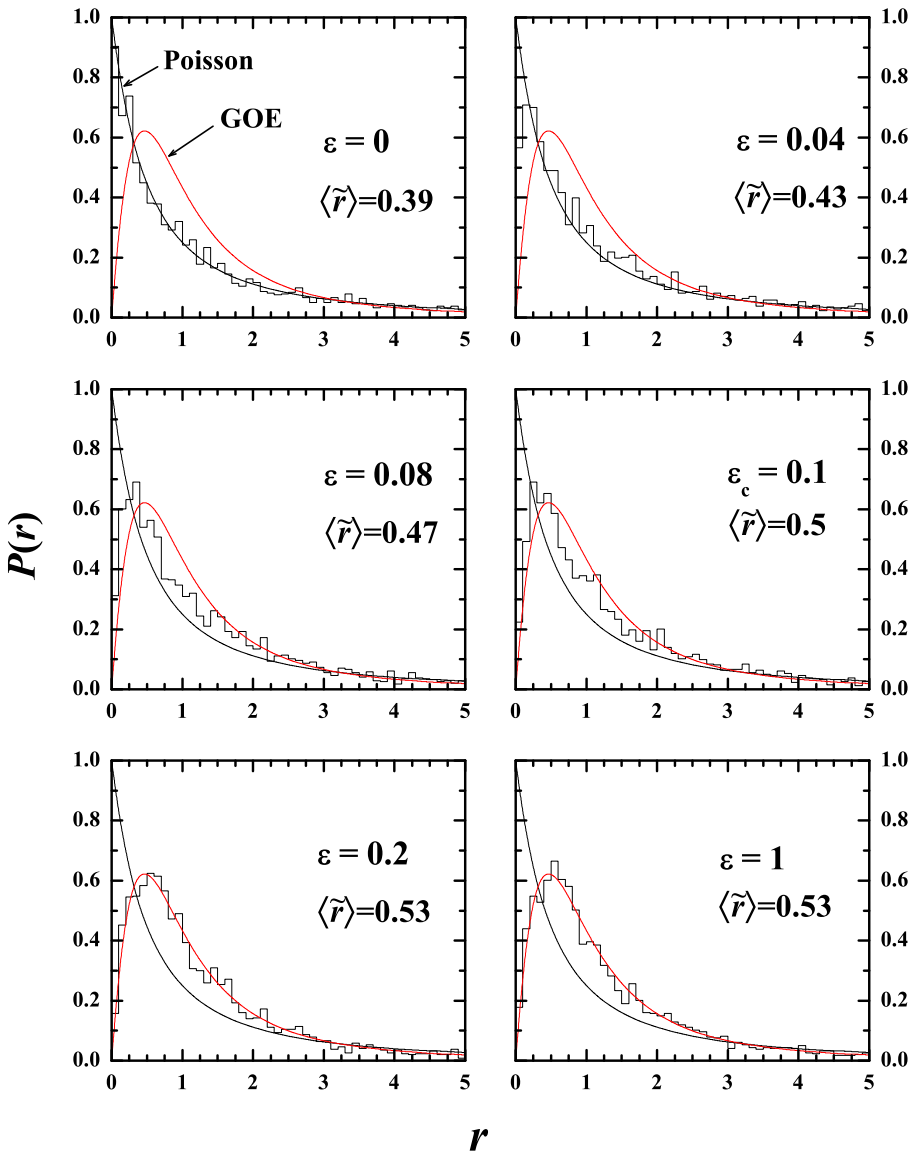

Figure 6.7: Histograms represent $P(r)$ distribution for Heisenberg's XXX model with $L = 14$ and 7 excitations for various values of defect strength ε. The defect is on the site $d = 7$. The value of ω_n is set as 0 for all n and similarly, J value is set to be 1. Values of $\langle \tilde{r} \rangle$ are also given in the figure and $\langle \tilde{r} \rangle = 0.5$ gives value of chaos marker ε_c. Bin size equal to 0.1 is used for the histograms and the results are compared with Poisson and Wigner (GOE) predictions

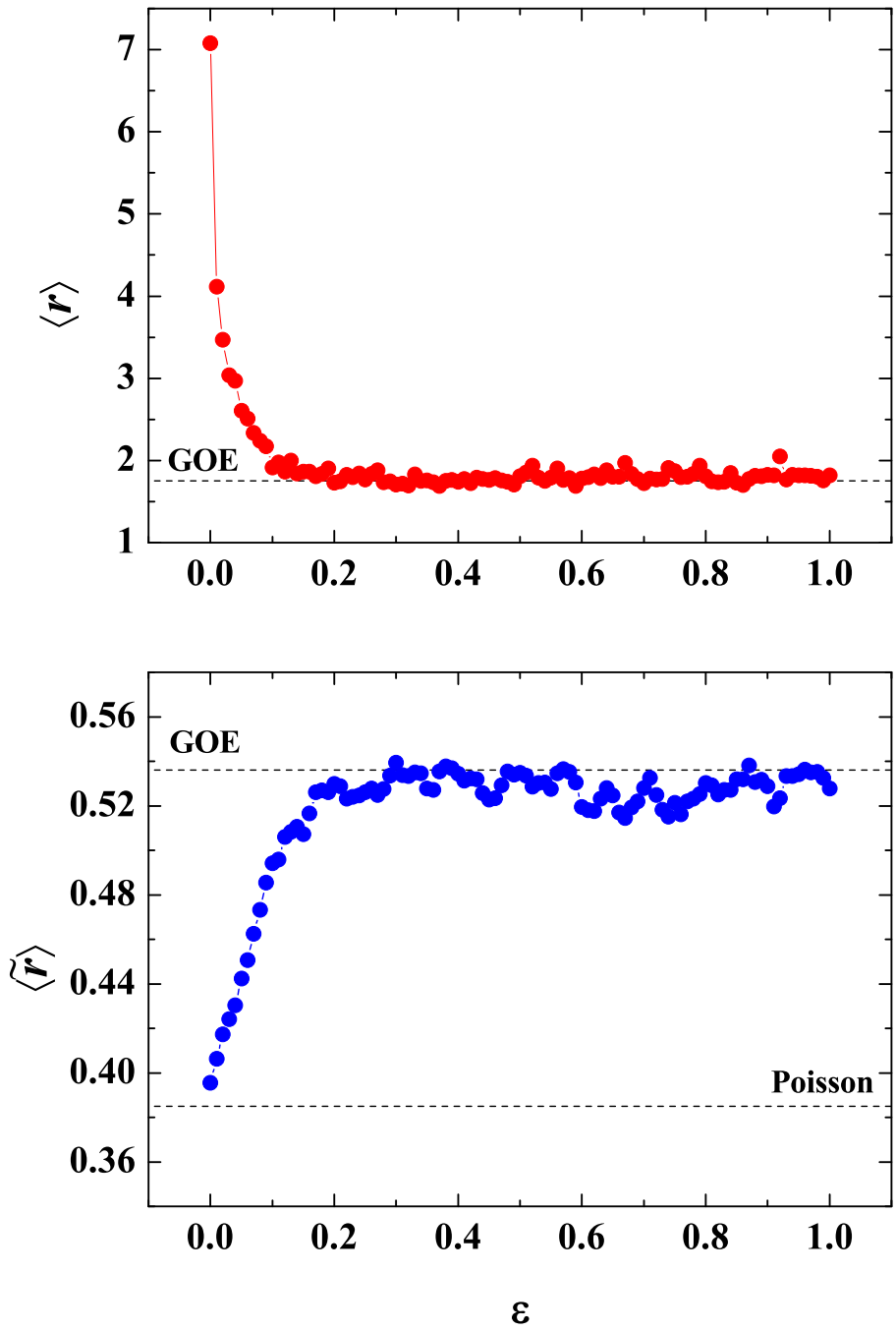

Figure 6.8: Variation of related averages $\langle r \rangle$ (upper panel) and $\langle \tilde{r} \rangle$ (lower panel) as a function of ε for Heisenberg's XXX model with L =14, 7 spins up and defect site d =7.

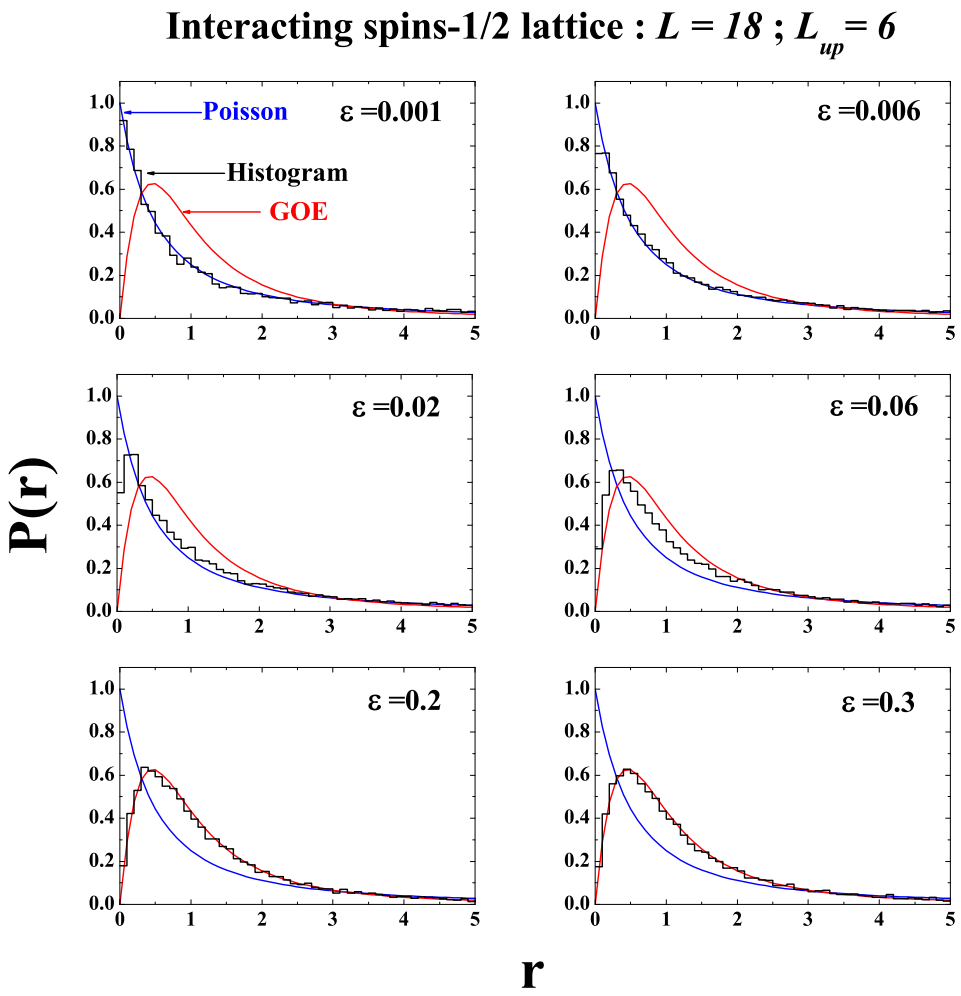

Figure 6.9: Histograms represent $P(r)$ distribution for Heisenberg's XXZ model with $L = 18$ and 6 excitations for various values of defect strength ε. The defect is on the site $d = 9$. The value of ω_n is set as 0 for all n and similarly, J_{xy} value is set to be 1 and J_z value is set as 0.5 and the results are compared with Poisson and Wigner (GOE) predictions

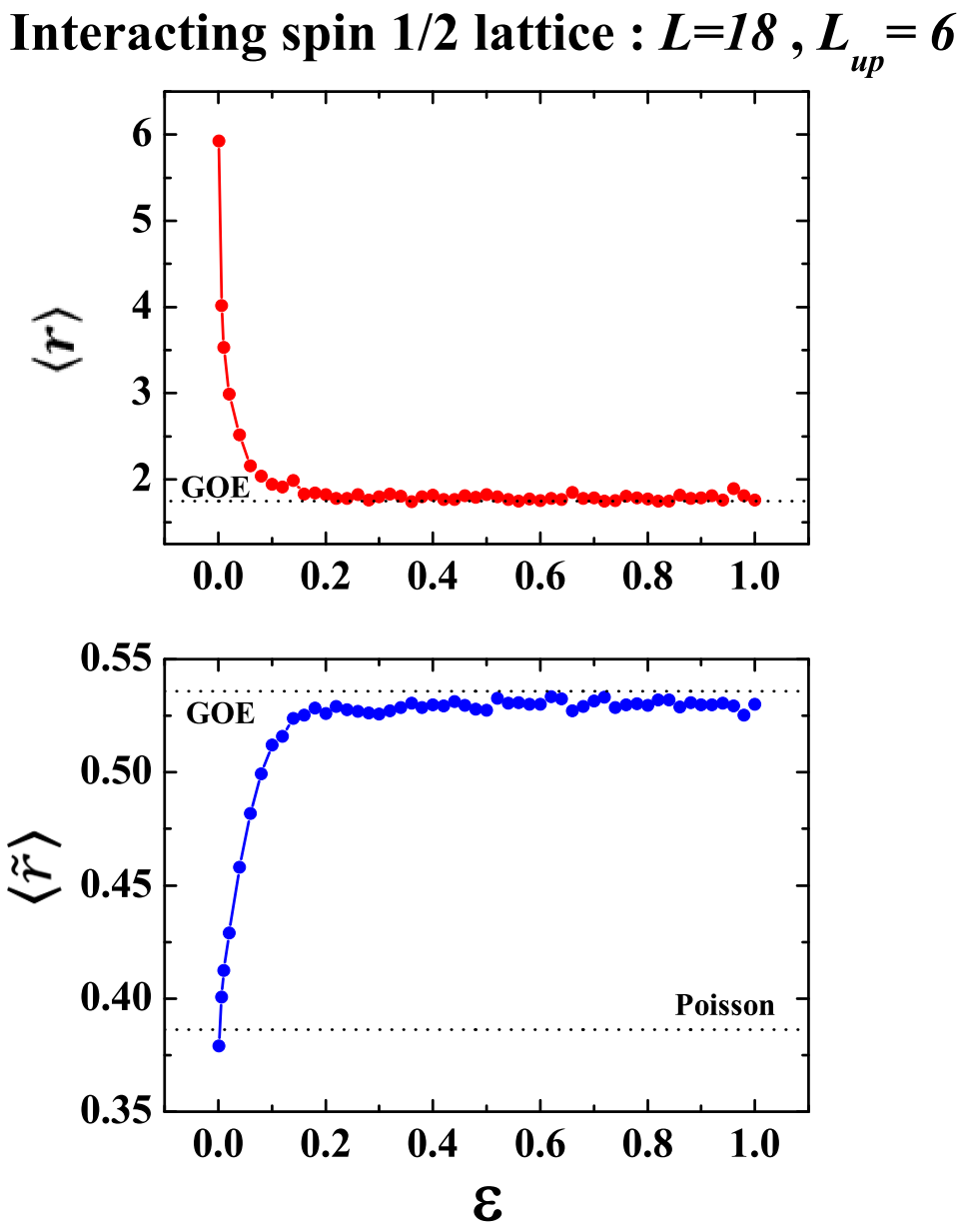

Figure 6.10: Variation of related averages $\langle r \rangle$ (upper panel) and $\langle \tilde{r} \rangle$ (lower panel) as a function of ε for Heisenberg's XXZ model with L =18, 6 spins up and defect site d =9.